Physics Letters B 693 (2010) 509–514

Contents lists available at ScienceDirect

Physics Letters B

www.elsevier.com/locate/physletb

Constraints on dark energy from the lookback time versus redshift test

Lado Samushia [a,b,*], Abha Dev [c], Deepa[...]

[a] Department of Physics, Kansas State University, 116 Cardwell Hall, Manhattan, KS 66506, USA
[b] National Abastumani Astrophysical Observatory, Ilia Chavchavadze University, 2A Kazbegi Ave, Tbilisi GE-0160, Georgia
[c] Miranda House, University of Delhi, Delhi 110 007, India
[d] Deen Dayal Upadhyaya College, University of Delhi, New Delhi 110 015, India

ARTICLE INFO

Article history:
Received 21 December 2009
Received in revised form 30 July 2010
Accepted 30 July 2010
Available online 5 August 2010
Editor: W.-D. Schlatter

Keywords:
Cosmological parameters
Galaxies, general
Galaxies, clusters, general
Galaxies, clusters, ages

ABSTRACT

We use lookback time versus redshift data from galaxy clusters (Capozziello et al., 2004 [9]) and passively evolving galaxies (Simon et al., 2005 [62]), and apply a Bayesian prior on the total age of the Universe based on WMAP measurements, to constrain dark energy cosmological model parameters. Current lookback time data provide interesting and moderately restrictive constraints on cosmological parameters. When used jointly with current baryon acoustic peak and Type Ia supernovae apparent magnitude versus redshift data, lookback time data tighten the constraints on parameters and favor slightly smaller values of the nonrelativistic matter energy density.

1. Introduction

It is now a well established fact that the expansion of the Universe is accelerating, but the underlying mechanism which gives rise to this cosmic acceleration is still a mystery. Recent cosmological observations including the Hubble diagram of Type Ia supernovae (SNeIa, e.g., [28,61,27]), combined with cosmic microwave background (CMB) anisotropy measurements (e.g., [20,33]), baryon acoustic peak galaxy power spectrum data (e.g., [44,57,26,66]), and galaxy cluster gas mass fraction measurements (e.g., [2,56,22]) indicate that we live in a spatially-flat Universe where nonrelativistic matter contributes about 30% of the critical density. Within the framework of Einstein's general theory of relativity, the rest of the 70% of the energy density of the Universe is termed dark energy, a mysterious component with negative effective pressure that is responsible for the observed accelerated expansion.[1] For recent reviews of dark energy see [51,8,24], and [53].

There are many dark energy candidates. The simplest is Einstein's cosmological constant Λ. In addition, there are other options like XCDM, a slowly rolling scalar field, Chaplygin gas, etc., which can also give rise to an accelerated expansion of the Universe. In this Letter we constrain the parameters of three different dark energy models. The first model is the cosmological constant dominated cold dark matter (ΛCDM) model [41]. In this model the energy density of the vacuum (the cosmological constant) does not vary with time and it has a negative pressure characterized by $p_\Lambda = -\rho_\Lambda$, where ρ_Λ is the vacuum energy density.

Secondly, we consider the XCDM parameterization of dark energy. In this case dark energy is assumed to be a fluid satisfying the following relation between pressure and the energy density, $p_\mathrm{x} = \omega_\mathrm{x}\rho_\mathrm{x}$, with $\omega_\mathrm{x} < 0$; this is not a physically complete model. Lastly, we study the slowly rolling dark energy scalar field ϕ model (ϕCDM) with an inverse power-law potential energy density for the scalar field, $V \propto \phi^{-\alpha}$ where α is a nonnegative constant [42,50,43].[2] We only consider the spatially-flat ϕCDM and XCDM cases. The ϕCDM model with $\alpha = 0$ and the XCDM model with $\omega_\mathrm{x} = -1$ are equivalent to the spatially-flat ΛCDM model with the same matter density. In all three models the nonrelativistic matter density is dominated by cold dark matter.

In this Letter we use two sets of lookback time versus redshift measurements, for galaxy clusters [9] and for passively evolving galaxies [62], and apply a Bayesian prior on the total age of the

* Corresponding author at: Department of Physics, Kansas State University, 116 Cardwell Hall, Manhattan, KS 66506, USA.

E-mail addresses: lado@phys.ksu.edu (L. Samushia), abha_dev@yahoo.com (A. Dev), djain@ddu.du.ac.in (D. Jain), ratra@phys.ksu.edu (B. Ratra).

[1] For discussions of modification of Einsteinian gravity on cosmological scales that attempt to do away with the need for dark energy, see [49,5,10,70,72], and references therein.

[2] In the ϕCDM model we consider here, ϕ only couples gravitationally to other components. For models where ϕ also interacts more directly with other components, see [15,4,7,45,25,35], and references therein. For other dark energy models, see [39,3,29,6,63,21,40], and references therein.

0370-2693
doi:10.1016/j.physletb.2010.07.057

Universe based on WMAP estimates [20], to constrain parameters of these dark energy models. This time-based cosmological test differs from other widely-used distance-based cosmological tests.[3] An important feature of this time-based method is that the age of distant objects are independent of each other. Therefore, it may avoid biases that are present in techniques that use distances of primary or secondary indicators in the cosmic distance ladder method. In the literature a variety of time-based methods have been considered, based on measurements of the absolute age of objects, differential age of objects, and lookback time of objects.[4]

The absolute age method is based on the simple criterion that the age of the Universe at a given redshift is always greater than or equal to the age of the oldest object at that redshift [1,37,30,67]. The differential age method is based on the measurement of $\Delta z/\Delta t$. Δz is the redshift separation between the two passively evolving galaxies having the age difference Δt [31,32]. This method requires a large sample of passively evolving galaxies with high quality spectroscopy and is probably more reliable than the absolute age method as a number of systematic effects are eliminated.

Lookback time as a tool to constrain dark energy models was first used by Capozziello et al. [9] who compiled a list of galaxy cluster ages and redshifts and used this data to constrain the XCDM dark energy parameterization. This data has been used to constrain brane cosmology and holographic dark energy models [46,71]. The lookback time test has also been applied using passively evolving galaxies data, to constrain parameters of XCDM and ΛCDM [17,18]. No doubt these time-based methods are subject to some different systematic errors but they offer an independent means to cross-check cosmological constraints obtained using other techniques.

In this Letter we take advantage of the fact that the [9] galaxy cluster data and the [62] passive galaxy data are independent, so it is straightforward to use them simultaneously in a lookback time versus redshift test analysis of dark energy models. Our joint analyses of these data sets allow us to derive the tightest lookback time constraints on dark energy parameters to date. The resulting constraints are moderately restrictive, and these data favor lower matter density values than do some other current data, but are consistent with a spatially-flat ΛCDM model in which nonrelativistic matter contributes 30% of the energy budget at a little less than two standard deviations. To derive tighter constraints, we perform a joint analysis of the lookback time data with current baryon acoustic peak and SNeIa measurements.

In Section 2 we describe the lookback time as a function of redshift test. The data and method we use are outlined in Section 3. Our results are presented and discussed in Section 4.

2. Lookback time versus redshift test

The lookback time is the difference between the present age of the Universe (t_0) and its age at redshift z, $t(z)$,

$$\begin{aligned} t_L(z,p) &= t_0(p) - t(z) \\ &= \frac{1}{H_0}\left[\int_0^\infty \frac{dz'}{(1+z')\mathcal{H}(z',p)} - \int_z^\infty \frac{dz'}{(1+z')\mathcal{H}(z',p)}\right] \\ &= \frac{1}{H_0}\int_0^z \frac{dz'}{(1+z')\mathcal{H}(z',p)}. \end{aligned} \tag{1}$$

Here p are the parameters of the cosmological model under consideration, $\mathcal{H}(z,p) = H(z,p)/H_0$, $H(z,p)$ is the Hubble parameter at redshift z, and the Hubble constant $H_0 = 100h\ \mathrm{km\,s^{-1}\,Mpc^{-1}}$.

Following [9], the observed lookback time $t_L^{\mathrm{obs}}(z_i)$, to an object i at redshift z_i is defined as

$$t_L^{\mathrm{obs}}\big(z_i, t_{\mathrm{inc}}, t_0^{\mathrm{obs}}\big) = t_0^{\mathrm{obs}} - t_i(z_i) - t_{\mathrm{inc}}. \tag{2}$$

Here

- t_0^{obs} is the measured current age of the Universe.
- $t_i(z_i)$ is the age of the object (passively evolving galaxy, cluster, etc.), defined as the difference between the current age of the Universe at redshift z_i and the age of the Universe when the object was born at redshift z_f,

$$\begin{aligned} t_i(z_i) &= t(z_i) - t(z_f) = t_L(z_f) - t_L(z_i) \\ &= \frac{1}{H_0}\int_{z_i}^{z_f} \frac{dz'}{(1+z')\mathcal{H}(z',p)}, \end{aligned} \tag{3}$$

  where we have used Eq. (1).
- $t_{\mathrm{inc}} = t_0^{\mathrm{obs}} - t_L(z_f)$ is the incubation time of the object. This delay factor encodes our ignorance of the formation redshift z_f.

To compute model predictions for the lookback time $t_L(z,p)$, Eq. (1), we need an expression for $H(z,p)$. In the ΛCDM model the Hubble parameter is

$$\begin{aligned} H(z,p) = H_0\big[&\Omega_{\mathrm{m}}(1+z)^3 \\ &+ (1-\Omega_{\mathrm{m}}-\Omega_\Lambda)(1+z)^2 + \Omega_\Lambda\big]^{1/2}, \end{aligned} \tag{4}$$

where p are Ω_{m} and Ω_Λ, the nonrelativistic matter and dark energy density parameters at $z=0$. For the XCDM parameterization in a spatially-flat cosmological model we have

$$H(z,p) = H_0\big[\Omega_{\mathrm{m}}(1+z)^3 + (1-\Omega_{\mathrm{m}})(1+z)^{3(1+\omega_{\mathrm{x}})}\big]^{1/2}, \tag{5}$$

where p are Ω_{m} and ω_{x}. In the spatially-flat ϕCDM model

$$H(z,p) = H_0\big[\Omega_{\mathrm{m}}(1+z)^3 + \Omega_\phi(z)\big]^{1/2}, \tag{6}$$

where the scalar field energy density parameter $\Omega_\phi(z)$ can be evaluated numerically by solving the coupled set of equations of motion,

$$\ddot\phi + 3\frac{\dot a}{a}\dot\phi - \frac{\kappa\alpha}{2}m_p^2\phi^{-(\alpha+1)} = 0, \tag{7}$$

$$\left(\frac{\dot a}{a}\right)^2 = \frac{8\pi}{3m_p^2}\big[\Omega_{\mathrm{m}}(1+z)^3 + \Omega_\phi(z)\big], \tag{8}$$

$$\Omega_\phi(z) = \big[(\dot\phi)^2 + \kappa m_p^2\phi^{-\alpha}\big]/12. \tag{9}$$

Here $a(t)$ is the scale factor, an overdot denotes a time derivative, m_p is Planck's mass, and κ and α are nonnegative constants that characterize the inverse power law potential energy density of the scalar field, $V(\phi) = \kappa\phi^{-\alpha}$. In this case the parameters p are Ω_{m} and α.

[3] Distance-based cosmological tests include those mentioned above that use SNeIa, CMB, baryon acoustic peak, and galaxy cluster gas mass fraction data, as well as radio-galaxy and quasar angular size versus redshift data (e.g., [13,47,16,60]) and gamma-ray burst luminosity distance versus redshift measurements (e.g., [64,48,68,36,65,59]).

[4] A variation of this test uses measurements of the Hubble parameter as a function of redshift (e.g., [55,38,19,23], and references therein).

Table 1

[62] galaxy ages

z_i	$t_i(z_i)$ (Gyr)
0.1171	10.2
0.1174	10.0
0.2220	9.0
0.2311	9.0
0.3559	7.6
0.4520	6.8
0.5750	7.0
0.6440	6.0
0.6760	6.0
0.8330	6.0
0.8360	5.8
0.9220	5.5
1.179	4.6
1.222	3.5
1.224	4.3
1.225	3.5
1.226	3.5
1.340	3.4
1.380	3.5
1.383	3.5
1.396	3.6
1.430	3.2
1.450	3.2
1.488	3.0
1.490	3.6
1.493	3.2
1.510	2.8
1.550	3.0
1.576	2.5
1.642	3.0
1.725	2.6
1.845	2.5

3. Data and computation

In order to constrain cosmological parameters of ΛCDM, XCDM, and ϕCDM, we use two age data sets. One is the [62] ages of 32 passively evolving galaxies (Table 1, [73]) in the redshift interval $0.117 \leqslant z \leqslant 1.845$. For this sample we assume a 12% one standard deviation uncertainty on the age measurements [73]. The other is [9, Table 1] ages of 6 galaxy clusters in the redshift range $0.10 \leqslant z \leqslant 1.27$. This sample has a 1 Gyr one standard deviation uncertainty on the age measurements. In all, we have 38 measurements of $t_L^{\rm obs}(z_i)$ with uncorrelated uncertainties σ_i.

For each model and parameter value set (p) we compute the χ^2 function

$$\chi^2\big(p, H_0, t_{\rm inc}, t_0^{\rm obs}\big) = \sum_{i=1}^{38} \frac{(t_{\rm L}(z_i, p) - t_{\rm L}^{\rm obs}(z_i, t_{\rm inc}, t_0^{\rm obs}))^2}{\sigma_i^2 + \sigma_{t_0^{\rm obs}}^2} + \frac{(t_0(p, H_0) - t_0^{\rm obs})^2}{\sigma_{t_0^{\rm obs}}^2}, \tag{10}$$

where $\sigma_{t_0}^{\rm obs}$ is the uncertainty in the estimate of t_0 and $t_L(z_i, p)$ and $t_0(p)$ are the predicted values in the model under consideration. From χ^2 we construct a likelihood function $\mathcal{L}'(p, H_0, t_{\rm inc}) \propto \exp(-\chi^2/2)$.

The likelihood function $\mathcal{L}'(p, H_0, t_{\rm inc}, t_0^{\rm obs})$ depends on the total age of the Universe $t_0^{\rm obs}$, incubation time $t_{\rm inc}$ and the Hubble parameter H_0. We do not know $t_{\rm inc}$ and so treat it as a nuisance parameter and analytically marginalize $\mathcal{L}'$ over it as in [9,17]. We treat H_0 as a nuisance parameter and marginalize over it with a Gaussian prior with $h = 0.742 \pm 0.036$ [52], a little higher than, but still consistent with, the earlier summary value of $h = 0.68 \pm 0.04$ [12]. We also apply a Bayesian prior as a Gaussian function with central values and variances based on the WMAP estimate of the total age of the Universe, which is $t_0^{\rm obs} = (13.75 \pm 0.13)$ Gyr for the ΛCDM model and $t_0^{\rm obs} = (13.75^{+0.29}_{-0.27})$ Gyr for the XCDM model [20].[5] For the ϕCDM model we assume the same central value as the other two models and conservatively inflate the error bar to $t_0^{\rm obs} = (13.75 \pm 0.5)$ Gyr. The resulting lookback time likelihood function depends only on the two cosmological parameters p, $\mathcal{L}_L(p)$. The best-fit parameters are the pair p^* that maximize the likelihood function and the 1, 2, and 3σ confidence level contours are defined as the sets of cosmological parameters p_σ at which the likelihood $\mathcal{L}(p_\sigma)$ is $\exp(-2.30/2)$, $\exp(-6.18/2)$, and $\exp(-11.83/2)$ times smaller than the maximum likelihood $\mathcal{L}(p^*)$.

To check our method we used the [9] galaxy cluster data and the earlier $t_0^{\rm obs}$ result they used and computed the constraints on the XCDM parameterization. Our contours are consistent with those shown in Fig. 2 of [9]. We also used the [62] passively evolving galaxy ages and the $t_0^{\rm obs}$ value [17] used to constrain the ΛCDM model. We find that if we pick $h = 0.72$ we are able to accurately reproduce the central and right panels of Fig. 2 of [17].

The lookback time versus redshift data constraints on ΛCDM, XCDM, and ϕCDM are shown in Figs. 1–3.

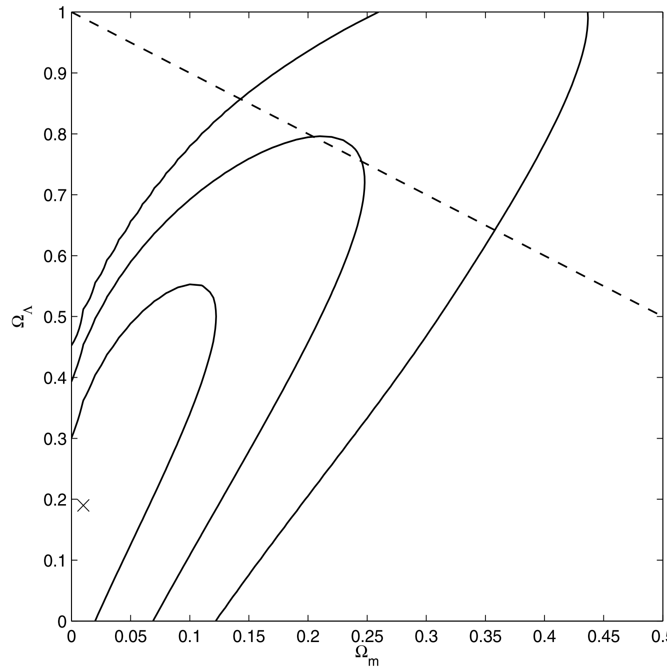

Fig. 1. 1, 2, and 3σ confidence level contours for the ΛCDM model from the lookback time data and measurement of the age of the Universe. The dashed line corresponds to spatially-flat models. The cross indicates the best-fit parameters $\Omega_{\rm m} = 0.01$ and $\Omega_\Lambda = 0.19$ with $\chi^2 = 33$ for 37 degrees of freedom.

4. Results and discussions

Fig. 1 shows the constraints on the ΛCDM model from the lookback time and age of the Universe measurements. The data favor low vales of both $\Omega_{\rm m}$ and Ω_Λ with the best-fit values being $\Omega_{\rm m} = 0.01$ and $\Omega_\Lambda = 0.19$. These data prefer spatially-open models, however a spatially-flat ΛCDM model with $\Omega_{\rm m} = 0.3$ is less than 3σ from the best-fit model. The data constrains $\Omega_{\rm m}$ to be less than 0.45 on 3σ confidence level.

[5] The numbers are taken from http://gsfc.nasa.gov/.

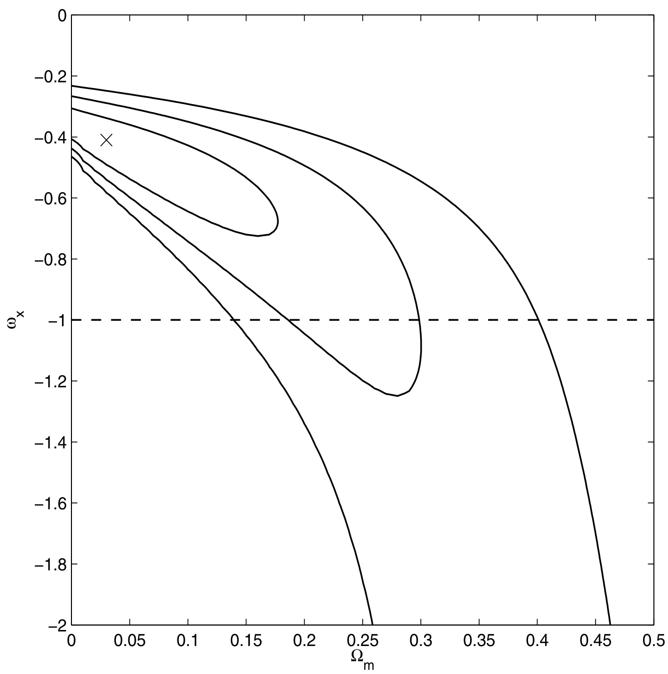

Fig. 2. 1, 2, and 3σ confidence level contours for the XCDM parameterization of dark energy in a spatially-flat cosmological model, from the lookback time data and measurement of the age of the Universe. The dashed $\omega_x = -1$ line corresponds to spatially-flat ΛCDM models. The cross indicates the best-fit parameters $\Omega_m = 0.03$ and $\omega_x = -0.41$ with $\chi^2 = 28$ for 37 degrees of freedom.

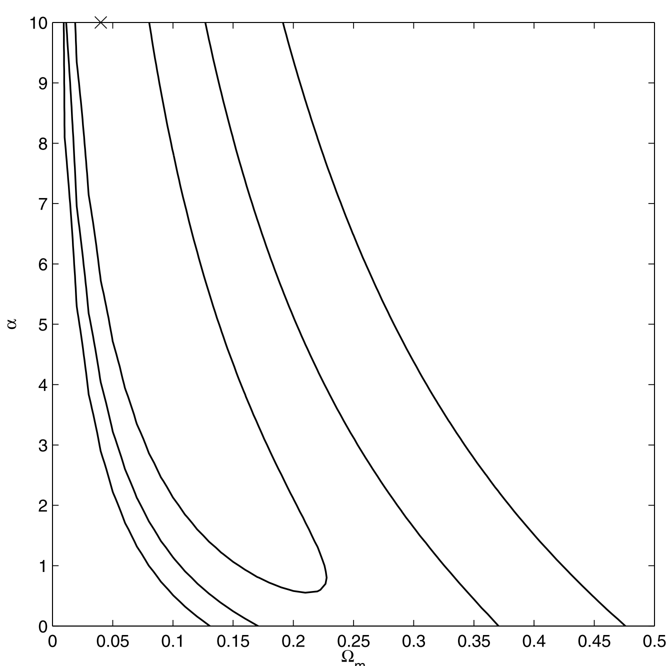

Fig. 3. 1, 2, and 3σ confidence level contours for the spatially-flat ϕCDM model from the lookback time data and measurement of the age of the Universe. The $\alpha = 0$ horizontal axis corresponds to spatially-flat ΛCDM models. The cross indicates the best-fit parameters $\Omega_m = 0.04$ and $\alpha = 10$ with $\chi^2 = 22$ for 37 degrees of freedom.

Fig. 2 presents the constraints on the XCDM parametrization of the equation of state. The nonrelativistic matter density parameter is constrained to be less than 0.5 at 3σ confidence. Low values of Ω_m are favored with the best-fit values being $\Omega_m = 0.03$ and $\omega_x = -0.41$ and a spatially-flat model with $\Omega_m = 0.3$ is about 2σ from the best-fit model.

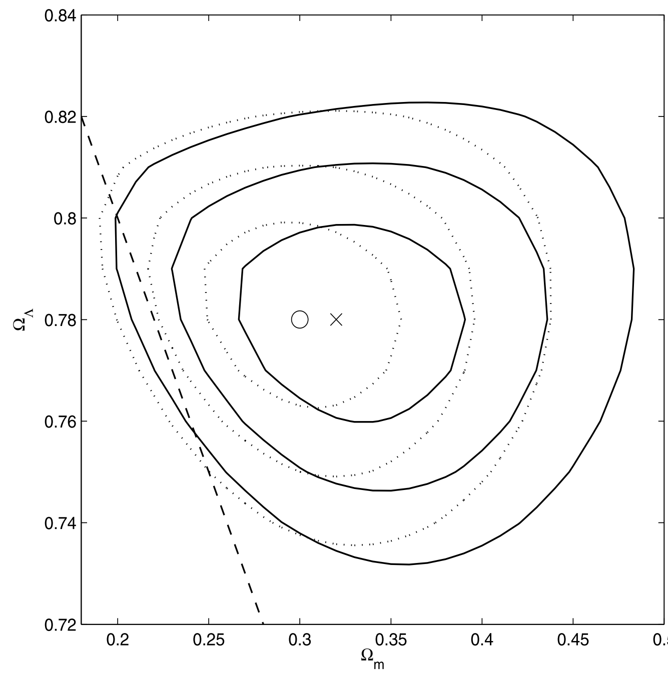

Fig. 4. 1, 2, and 3σ confidence level contours for the ΛCDM model. Numerical noise is responsible for the jaggedness of parts of the contours. The dashed line demarcates spatially-flat models. Dotted lines (circle denotes the best-fit point at $\Omega_m = 0.30$ and $\Omega_\Lambda = 0.78$ with $\chi^2 = 359$ for 346 degrees of freedom) are derived using the lookback time data, measurement of the age of the Universe, SNeIa Union data, and BAO peak measurements, while solid lines (cross denotes the best-fit point at $\Omega_m = 0.32$ and $\Omega_\Lambda = 0.78$ with $\chi^2 = 318$ for 307 degrees of freedom) are derived using SNeIa and BAO data. The dashed line corresponds to spatially-flat models.

Fig. 3 shows the constraints on the ϕCDM model of dark energy. In this model the nonrelativistic matter density parameter is less than 0.5 at 3σ confidence. The α parameter on the other hand is not well constrained. The best-fit parameter value is $\alpha = 10$, but the likelihood is very flat in the direction of α and the difference between the best-fit value and $\alpha = 0$ (which is the spatially-flat ΛCDM case) is slightly less than 2σ.

Current lookback time data by themselves are unable to tightly constrain cosmological parameters. Constraints from galaxy cluster gas mass fraction versus redshift data (e.g., [14]), SNeIa apparent magnitude versus redshift measurements (e.g., [69]), and baryon acoustic peak data (e.g., [58]) are more restrictive than the lookback time constraints. However, the constraints from lookback time data are somewhat tighter than the constraints from strong gravitational lensing data (e.g., [11]), measurements of the Hubble parameter as a function of redshift (e.g., [54]), radio galaxy angular size versus redshift data (e.g., [16]), and gamma-ray burst luminosity distance versus redshift data (e.g., [59]).

To get tighter constraints on cosmological parameters we combine the lookback time data and the measurement of the age of the Universe with baryon acoustic peak data [44] and SNeIa "Union" apparent magnitude versus redshift measurements [34]. Since these data sets are independent we compute a joint likelihood function that is a product of individual likelihood functions

$$\mathcal{L}_{\rm joint} = \mathcal{L}_L \mathcal{L}_{\rm BAO} \mathcal{L}_{\rm SNe}, \tag{11}$$

and define the best-fit parameters and confidence level contours as discussed above.

The constraints on the three dark energy models from a joint analysis of these data are shown in Figs. 4–6. Currently available lookback time data do not significantly change the results derived

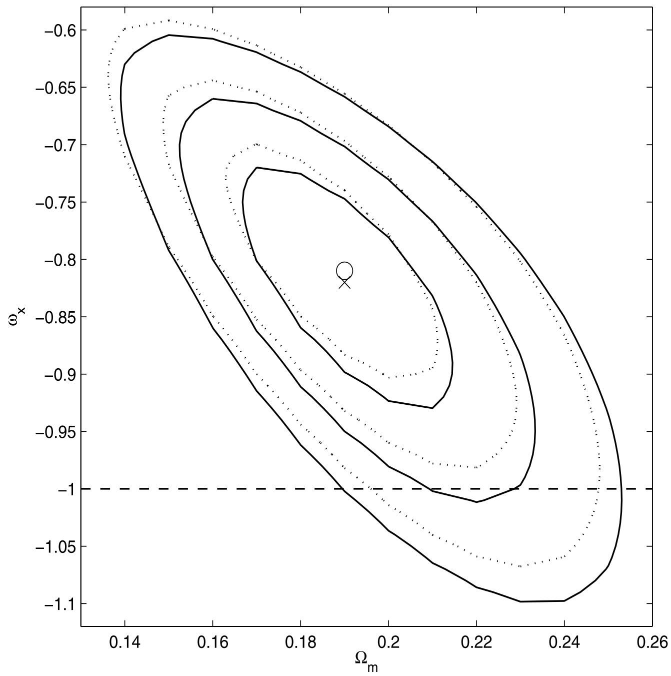

Fig. 5. 1, 2, and 3σ confidence level contours for the XCDM parameterization of dark energy in a spatially-flat cosmological model. The dashed line demarcates spatially-flat ΛCDM models. Dotted lines (circle denotes the best-fit point at $\Omega_m = 0.19$ and $\omega_x = -0.80$ with $\chi^2 = 352$ for 346 degrees of freedom) are derived using the lookback time data, measurement of the age of the Universe, SNeIa Union data, and BAO peak measurements, while solid lines (cross denotes the best-fit point at $\Omega_m = 0.19$ and $\omega_x = -0.81$ with $\chi^2 = 321$ for 307 degrees of freedom) are derived using only SNeIa and BAO data. The dashed ω_x line corresponds to spatially-flat ΛCDM models.

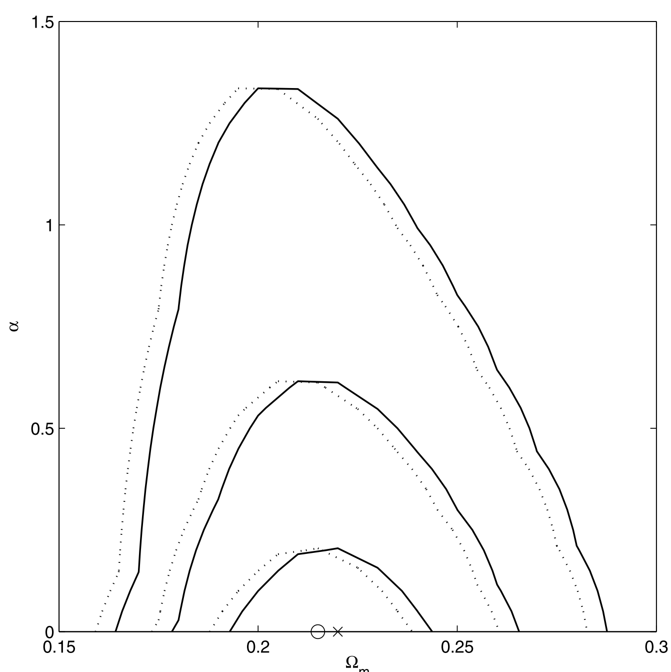

Fig. 6. 1, 2, and 3σ confidence level contours for the spatially-flat ϕCDM model. The $\alpha = 0$ horizontal axis corresponds to spatially-flat ΛCDM models. Dotted lines (circle denotes the best-fit point at $\Omega_m = 0.215$ and $\alpha = 0.0$ with $\chi^2 = 359$ for 346 degrees of freedom) are derived using the lookback time data, measurement of the age of the Universe, SNeIa Union data, and BAO peak measurements, while solid lines (cross denotes the best-fit point at $\Omega_m = 0.22$ and $\alpha = 0.0$ with $\chi^2 = 329$ for 307 degrees of freedom) are derived using only SNeIa and BAO data.

using BAO peak measurements and SNeIa apparent magnitude data. In all three dark energy models when lookback time data are added to the mix the confidence level regions favor slightly smaller values of nonrelativistic matter density parameter Ω_m.

Overall, current data is a good fit to all three dark energy models. For ϕCDM and XCDM they slightly favor time-dependent dark energy, but the time-independent cosmological constant is also a good fit.

We anticipate that a new, improved data set of lookback times will soon be available [74]. With more and better data we expect significantly tighter constraints on dark energy parameters. The lookback time versus redshift test, either by itself or at least in combination with other cosmological probes, could prove very useful in detecting or constraining dark energy time evolution.

Acknowledgements

Abha Dev and Deepak Jain thank A. Mukherjee and S. Mahajan for providing facilities to carry out this research. Deepak Jain acknowledges the hospitality provided by the IUCAA, Pune where the part of the work is done. D.J. and A.D. acknowledge the financial support provided by Department of Science and Technology, Govt. of India under project No. SR/S2/HEP-002/2008. We acknowledge support from DOE grant DE-FG03-99EP41093, Georgian National Science foundation grant ST08/4-442, and Scientific Co-operation Programme between Eastern Europe and Switzerland (SCOPES) grant.

References

[1] J.S. Alcaniz, J.A.S. Lima, ApJ 521 (1999) L87.
[2] S.W. Allen, et al., MNRAS 383 (2008) 879.
[3] A. Arbey, Open Astron. J. 1 (2008) 27.
[4] M. Baldi, V. Pettorino, G. Robbers, V. Springel, arXiv:0812.3901 [astro-ph], 2009.
[5] K. Bamba, C.-Q. Geng, Phys. Lett. B 679 (2009) 282.
[6] S. Basilakos, arXiv:0901.3195 [astro-ph.CO], 2009.
[7] M.C. Bento, Felipe González, Phys. Lett. B 674 (2009) 146.
[8] R.R. Caldwell, M. Kamionkowski, Annu. Rev. Nucl. Part. Sci. 59 (2009) 397.
[9] S. Capozziello, et al., Phys. Rev. D 70 (2004) 123501.
[10] S. Capozziello, V. Salzano, arXiv:0902.0088 [astro-ph.CO], 2009.
[11] K.-H. Chae, G. Chen, B. Ratra, D.-W. Lee, ApJ 607 (2004) L71.
[12] G. Chen, J.R. Gott, B. Ratra, PASP 115 (2003) 1269.
[13] G. Chen, B. Ratra, ApJ 582 (2003) 586.
[14] G. Chen, B. Ratra, ApJ 612 (2004) L1.
[15] X.-M. Chen, Y. Gong, E.N. Saridakis, JCAP 0904 (2009) 001.
[16] R.A. Daly, et al., ApJ 691 (2009) 1058.
[17] M.A. Dantas, J.S. Alcaniz, D. Jain, A. Dev, A&A 467 (2007) 421.
[18] M.A. Dantas, J.S. Alcaniz, N. Pires, Phys. Lett. B 679 (2009) 423.
[19] A. Dev, D. Jain, D. Lohiya, arXiv:0804.3491 [astro-ph], 2008.
[20] J. Dunkley, et al., Astrophys. J. Suppl. 180 (2009) 306.
[21] S. Dutta, R.J. Scherrer, Phys. Lett. B 676 (2009) 12.
[22] S. Ettori, et al., arXiv:0904.2740 [astro-ph.CO], 2009.
[23] E. Fernandez-Martinez, L. Verde, JCAP 0808 (2008) 023.
[24] J.A. Frieman, arXiv:0904.1832 [astro-ph.CO], 2009.
[25] M.B. Gavela, et al., JCAP 0907 (2009) 034.
[26] E. Gaztañaga, A. Cabré, L. Hui, arXiv:0807.3551 [astro-ph], 2009.
[27] A.C.C. Guimarães, J.V. Cunha, J.A.S. Lima, JCAP 0910 (2009) 010.
[28] M. Hicken, et al., ApJ 700 (2009) 1097.
[29] O. Hrycyna, M. Szydłowski, JCAP 04 (2009) 026.
[30] D. Jain, A. Dev, Phys. Lett. B 633 (2006) 436.
[31] R. Jimenez, A. Loeb, ApJ 573 (2002) 37.
[32] R. Jimenez, L. Verde, T. Treu, D. Stern, ApJ 593 (2003) 622.
[33] E. Komatsu, et al., ApJS 180 (2009) 330.
[34] M. Kowalski, et al., ApJ 686 (2008) 749.
[35] G. La Vacca, et al., J. Cosmology, Astropart. Phys. 0904 (2009) 007.
[36] N. Liang, L.N. Zhang, AIP Conf. Proc. 1065 (2008) 367.
[37] J.A.S. Lima, J.S. Alcaniz, MNRAS 317 (2000) 893.
[38] H. Lin, et al., arXiv:0804.3135 [astro-ph], 2008.
[39] J. Lu, L. Xu, B. Chang, Y. Gui, Internat. J. Modern Phys. D 18 (2009) 1741.
[40] I.P. Neupane, H. Trowland, Internat. J. Modern Phys. D 19 (2009) 367.
[41] P.J.E. Peebles, ApJ 284 (1984) 439.
[42] P.J.E. Peebles, B. Ratra, ApJ 325 (1988) L17.
[43] P.J.E. Peebles, B. Ratra, Rev. Modern Phys. 75 (2003) 559.

[44] W.J. Percival, et al., MNRAS 381 (2007) 1053.
[45] V. Pettorino, D.F. Mota, G. Robbers, C. Wetterich, AIP Conf. Proc. 1115 (2009) 291.
[46] N. Pires, Z.-H. Zhu, J.S. Alcaniz, Phys. Rev. D 73 (2006) 123530.
[47] S. Podariu, R.A. Daly, M. Mory, B. Ratra, ApJ 584 (2003) 577.
[48] S. Qi, F.-Y. Wang, T. Lu, A&A 487 (2009) 853.
[49] D. Rapetti, S.W. Allen, A. Mantz, H. Ebeling, arXiv:0812.2259 [astro-ph], 2009.
[50] B. Ratra, P.J.E. Peebles, Phys. Rev. D 37 (1988) 3406.
[51] B. Ratra, M.S. Vogeley, PASP 120 (2008) 235.
[52] A.G. Riess, et al., ApJ 699 (2009) 539.
[53] M. Sami, Current Sci. 97 (2009) 887.
[54] L. Samushia, G. Chen, B. Ratra, arXiv:0706.1963 [astro-ph], 2007.
[55] L. Samushia, B. Ratra, ApJ 650 (2006) L5.
[56] L. Samushia, B. Ratra, ApJ 680 (2008) L1.
[57] L. Samushia, B. Ratra, ApJ 703 (2009) 1904.
[58] L. Samushia, B. Ratra, ApJ 701 (2009) 1373.
[59] L. Samushia, B. Ratra, ApJ 714 (2010) 1347.
[60] R.C. Santos, J.A.S. Lima, Phys. Rev. D 77 (2008) 083505.
[61] A. Shafieloo, V. Sahni, A.A. Starobinsky, PRD 80 (2009) 101301.
[62] J. Simon, L. Verde, R. Jimenez, Phys. Rev. D 71 (2005) 123001.
[63] S. Tsujikawa, T. Tamaki, R. Tavakol, JCAP 0905 (2009) 020.
[64] R. Tsutsui, et al., MNRAS 394 (2009) L31.
[65] Y. Wang, Phys. Rev. D 78 (2008) 123532.
[66] Y. Wang, arXiv:0904.2218 [astro-ph.CO], 2009.
[67] H. Wei, S.N. Zhang, Phys. Rev. D 76 (2007) 063003.
[68] H. Wei, S.N. Zhang, Eur. Phys. J. C 63 (2008) 139.
[69] K.M. Wilson, G. Chen, B. Ratra, Modern Phys. Lett. A 21 (2006) 2197.
[70] F. Wu, X. Chen, arXiv:0903.0385 [astro-ph.CO], 2009.
[71] Z.L. Yi, T.J. Zhang, Modern Phys. Lett. A 22 (2007) 41.
[72] S.-Y. Zhou, E.J. Copeland, P.M. Saffin, JCAP 0907 (2009) 009.
[73] R. Jimenez, private communication, 2007.
[74] R. Jimenez, private communication, 2009.